VEGF$_{165}$ promotes the osteolytic bone destruction of Ewing's sarcoma tumors by upregulating RANKL

Hui Guan, **Zhichao Zhou**, **Ying Cao**, **Xiaoping Duan**, and **Eugenie S. Kleinerman**
Division of Pediatrics, The University of Texas M. D. Anderson Cancer Center, Houston, Texas USA

Abstract

The purpose of this study was to determine whether vascular endothelial growth factor-165 (VEGF$_{165}$) contributed to the osteolytic process in Ewing's sarcoma. VEGF$_{165}$ induced osteoclast formation from murine bone marrow cells. Tartrate-resistant acid phosphatase (TRAP) staining demonstrated significantly fewer osteoclasts in VEGF-inhibited TC/siVEGF$_{7-1}$ tumors compared to TC71 parental or TC/si-control tumors. Receptor activator NF-κB (RANKL), a critical osteoclastogenic factor, was decreased in TC/siVEGF$_{7-1}$ cells. Incubation of these cells with recombinant VEGF$_{165}$ upregulated RANKL in a dose and time-dependent manner. The induction of (RANKL) by VEGF$_{165}$ was also demonstrated in MC3T3-E1 mouse osteoblast cells and bone marrow stromal cells. This upregulation was transcriptionally mediated by an effect on the RANKL promoter. Both VEGF and EWS/FLI-1 increased RANKL promoter activity. Taken together, these data suggest that modulation of RANKL by VEGF$_{165}$ may be one of the mechanisms responsible for the osteolytic process induced by Ewing's sarcoma cells. VEGF$_{165}$ may, therefore, play an important role in modulating RANKL gene expression in the bone marrow microenvironment during the metastatic process, thereby contribution to tumor induced bone lysis.

Keywords

VEGF$_{165}$; Ewing's sarcoma; RANKL; osteolysis

Introduction

Ewing's sarcoma, an aggressive bone tumor, affects children and young adults with a peak incidence at age 15. The most common sites of the primary tumor are the pelvis, long bones and bones of the chest wall (1). Despite multimodal treatment with surgery, chemotherapy and radiation the survival rates have plateaued at 50 – 60%, with no improvements in the past 20 years (2). Patients with metastatic disease at presentation have an even poorer outcome, with cure rates <30%. Understanding the biology of Ewing's sarcoma may therefore assist in the identification of new therapeutic targets for this disease.

Vascular endothelial growth factor (VEGF) has been shown to be critical for tumor vascular formation in numerous different malignancies, including Ewing's sarcoma (3). We have previously demonstrated that Ewing's sarcoma cell lines and primary patient tumor specimens overexpress the angiogenic factor VEGF with a shift in isoform from the membrane-bound 189 to the soluble 165 form (4). Inhibition of VEGF$_{165}$ with siRNA-inhibited tumor growth significantly decreased tumor vascularity and reduced tumor-induced bone lysis (5). In addition to being an angiogenesis factor, VEGF$_{165}$ also influences bone biology. In the skeleton, the

Correspondence: Eugenie S. Kleinerman, M.D., Division of Pediatrics, The University of Texas M. D. Anderson Cancer Center, 1515 Holcombe Boulevard, Unit 87, Houston, TX 77030. Phone: 713 792 8110; Fax: 713 794 5042. ekleiner@mail.mdanderson.org.

appearance of bone/cartilage resorbing cells coincides with blood vessel invasion and new vessel formation. VEGF has been shown to induce osteoclast migration, invasion and activation and supports the survival of mature osteoclasts (6–8). These processes play a key role in repairing and remodeling bone during bone development.

The role of VEGF in Ewing's sarcoma formation and tumor-induced bone lysis is unclear. Serum VEGF levels were significantly elevated in hepatocellular carcinoma patients with bone metastases compared to patients without bone metastases(9). Similar findings were reported in patients with giant cell bone sarcomas(10). We previously demonstrated that inhibition of $VEGF_{165}$ protein production by TC71 Ewing's sarcoma cells alters their lytic capacity *in vivo*, resulting in less tumor-induced bone destruction(5). These data support the hypothesis that tumor production of $VEGF_{165}$ contributes to osteolysis induced by tumor growth in the bone. The mechanism by which VEGF regulates osteolysis has not been determined.

Receptor activator NF-κB ligand (RANKL) is a cell-surface protein expressed on osteoblasts and bone marrow stromal cells (11;12) and is secreted by T lymphocytes and some cancer cells (13;14). RANKL interacts with the RANK receptor on osteoclast precursor cells promoting osteoclast differentiation and maturation in the bone microenvironment through cell-cell interaction. Many hormones, cytokines and growth factors stimulate osteoclast activity by regulating RANKL. Since we previously demonstrated that inhibiting $VEGF_{165}$ decreased the lytic activity of Ewing's sarcoma cells *in vivo* and RANKL stimulates osteoclastic activity, the purpose of this study was to investigate whether $VEGF_{165}$ promotes osteolysis by upregulating RANKL expression. Here we demonstrate that $VEGF_{165}$ induced murine bone marrow cells to differentiate into osteoclasts. $VEGF_{165}$ upregulated RANKL expression in osteoblasts, bone marrow stromal cells and Ewing's sarcoma tumor cells. This upregulation was transcriptionally mediated through an effect on the RANKL promoter. Specifically inhibiting $VEGF_{165}$ with siRNA resulted in decreased RANKL. Taken together, these results indicate that $VEGF_{165}$ may contribute to the osteolytic process induced by Ewing's sarcoma cells through a mechanism involving RANKL. This upregulation of RANKL may in turn increase osteoclastic activity in the tumor microenvironment, leading to bone lysis.

Material and Methods

Plasmid constructs

Specific VEGF siRNA-expressing plasmid was constructed as described previously (5). The 1879 bp region of the human RANKL gene upstream of the transcriptional starting site was amplified by polymerase chain reaction (PCR) using specific primers (RANKL, sense: 5'-agtcaaggagcagggagagaatgag-3', antisense: 5'-aggtacttggtgtagtctctg-3') from human Ewing's sarcoma TC71 cell genomic DNA and cloned between Kpn I and Xho I sites of pGL3-basic firefly luciferase reporter vector (Promega Corporation, Madison, WI).

Cell lines and transfection

TC71 human Ewing's sarcoma cells were cultured in Eagle's modified essential medium (EMEM; supplemented with 10% heat-inactivated fetal bovine serum (FBS), 1 mM sodium pyruvate, $2\times$ minimal essential medium vitamins, $1\times$ nonessential amino acids, and 2 mM glutamine) at 37°C, 5% CO_2 in a humidified incubator. Murine osteoblast MC3T3-E1, osteoclast-like RAW246.7cells, and fibroblast NIH3T3 cells were maintained in Dulbecco's modified eagle medium supplemented with 10% FBS. Murine bone marrow stromal cells were isolated from nude/nude mice bone marrow as described previously(15). Briefly, total bone marrow cells were collected from 2-month-old nude/nude mice (Charles River Breeding Laboratories, Kingston, MA) by flushing femoral bones with EMEM supplemented with 20% heat-inactivated FBS and penicillin/streptomycin (50 U/ml and 50 mg/ml, respectively; Gibco-

Invitrogen, Carlsbad, USA). Cells were then washed twice with medium and plated in a Petri dish at a density of 2×10^6 cells/cm^2. After 3 days, nonadherent cells were removed by 2 to 3 washes with phosphate-buffered saline (PBS). Adherent cells were further cultured in complete medium for 4 weeks. All cells were free of mycoplasma, as screened by Mycoplasma Plus PCR Primer Set (Stratagene Inc., La Jolla, CA), and verified to be free of pathogenic murine viruses (NCI-Frederick Cancer Research & Development Center, Frederick, MD). TC/siVEGF7-1 and TC/siVEGF7-17 cells were created by transfection of cells with VEGF165-siRNA (5) and maintained in hygromycin B (Invitrogen Life Technologies, Carlsbad, CA) containing medium at 400 μg/ml. These cells produce 98% less VEGF165 protein.

Histologic assessment and TRAP staining of bone

TC71, TC/si-, TC/siVEGF7-1 cells were intrabone injected into the tibias of nude mice as described previously(5). Bone tumors were collected 3 weeks later, fixed in 10% formalin for 24 h, and decalcified for 14 days using 10% EDTA (pH 7.4). The specimens were then paraffin embedded, cut into 5 μm sections, and stained with hematoxylin and eosin (H&E) for histologic assessment. To perform TRAP staining, non-stained sections were deparaffinized and rehydrated, then stained for TRAP. Briefly, the specimens were stained with sodium acetate and substrate Naphthol AS-BI phosphate (Sigma Chemical Co., St. Louis, MO) in the presence of tartaric acid for 30 min at 37°C, followed by 10 min color reaction incubation. Finally, the specimens were counterstained with hematoxylin.

In vitro *osteoclast formation assay and TRAP staining*

Murine bone marrow cells were collected aseptically from BALB/c mice. The collected cells were washed, resuspended in EMEM, supplemented with 10% FBS, and incubated at 37°C for 24 h. Following incubation, the nonadherent cells (hematopoietic cells) were collected and used in cultures as osteoclast precursors. The collected nonadherent hematopoietic cells were then plated onto 8-chamber slides (BD Biosciences, San Jose, CA) at a density of 5×10^5 cell/chamber alone or with NT3T3-E1 cells (1×10^4 cell/chamber) and cultured for 9 days in EMEM supplemented with 10% FBS with or without recombinant human VEGF (rhVEGF) at 50 ng/ml or recombinant human macrophage colony-stimulating factor (rhM-CSF) at 10 ng/ml. Half of the medium was changed every 3 days. After culturing for 9 days, the cells were fixed and stained for TRAP activity. TRAP-positive and multinucleated (>3 nuclei) cells were counted as osteoclast-like cells.

Western blot analysis

Cells were pipetted into 100-mm dishes. When cells reached 80% confluence, they were washed with cold PBS buffer, lysed in RIPA buffer (1% NP40, 0.5% sodium deoxycholate, and 0.1% sodium dodecylsulfate (SDS) in PBS) containing aprotinin (2 μg/ml), leupeptin (2 μg/ml), pepstatin A (1 μg/ml), and phenylmethylsulfonyl fluoride (100 μg/ml; Sigma), and then placed on ice for 30 min. Cells were centrifuged at 13,000 rpm for 10 min to eliminate cell debris. Protein concentrations were determined using the Bio-Rad protein assay kit (Bio-Rad Laboratories, Hercules, CA). The protein (50 μg) was boiled for 5 min before being loaded onto a 7.5% SDS-polyacrylamide gel and then transferred to a nitrocellulose membrane (Amersham, Little Chalfon, Buckinghamshire, UK). The specific protein bands were detected with anti-human RANKL (R&D Systems, Minneapolis, MN), anti-neuropilin (Santa Cruz Biotechnology, Santa Cruz, CA), anti-phospho-Erk (Cell Signaling Technology, Inc., Danvers, MA) and anti-ß-actin antibody (Sigma) using the ECL Western blotting analysis system (Amersham) according to the manufacturer's instructions. Densitometric analysis was performed, and values were normalized with ß-actin loading control.

Reverse transcription-PCR

Total RNA was extracted from different cells. The cDNA was synthesized using a Reverse Transcription System (Promega Corporation). Reverse transcription products were amplified by PCR (RT-PCR) using specific primers for murine RANKL (sense 5'-GGTCGGGCAATTCTGAATT-3'; antisense 5'-GGGAATTACAAAGTGCACCAG-3'). The initial denaturation was done at 94°C for 5 min. Followed by an additional denaturation at 94°C for 1 min, annealing at 58°C for 10 sec, extension at 72°C for 10 sec for 35 cycles, and a final elongation at 72°C for 10 min. The PCR products were subjected to electrophoresis on 1% agarose gel with ethidium bromide and visualized under ultraviolet light. The glyceraldehyde-3-phosphate dehydrogenase primers and competimers were used as the internal controls (sense 5'-GGTCGGGCAATTCTGAATT-3'; antisense 5'-GGGAATTACAAAGTGCACCAG-3').

Luciferase assay

The Promega Dual- Luciferase Reporter Assay System was used to assess luciferase activity (Promega Corporation). Briefly, reporter lysis buffer was added and incubated at room temperature for 15 min before centrifugation to remove cell debris. Twenty μl of cell lysate was mixed with 100 μl of luciferase substrate and light emission measured with the Monolight Luminometer (BD Biosciences). In each group, cell lysates were also measured for Renilla luciferase activity to allow for normalization of luciferase activity.

Immunohistochemical analysis

Tumor sections were stained with H&E. Cells cultured in chamber slides were fixed with acetone, incubated in 3% H_2O_2 in methanol for 10 min to block endogenous peroxidase, and then incubated in 5% normal horse serum plus 1% normal goat serum in PBS for 20 min to block nonspecific protein. The expression of VEGF receptor (VEGFR1) 1,VEGFR2 and phospho-VEGFR2 protein was detected by incubating slides with rabbit anti-VEGFR1 antibody (Santa Cruz Biotechnology), rabbit anti-VEGFR2 antibody (Santa Cruz Biotechnology), rabbit anti-phospho-VEGFR2 antibody (Merck Chemicals Ltd., San Diego, CA) as the primary antibody and horseradish peroxidase-labeled goat antibody against rabbit immunoglobulin G (IgG) as the second antibody (Jackson ImmunoResearch Laboratory, Inc., West Grove, PA). Gill's hematoxylin was used as a counterstain.

Results

Downregulation of VEGF$_{165}$ inhibits the osteolytic activity of TC71 cells in vivo

Histologic examination of the tibia from mice injected with TC71 and TC/si-control mice showed almost complete destruction of the cancellous and cortical bone with replacement by tumor cells (Fig. 1A). By contrast, although tumor cells were detected in the tibias from mice injected with TC/siVEGF$_{7-1}$ cells, the cortical bone remained intact and tumor cells did not invade into or destroy the bone cortex. These histologic findings confirmed our previous radiographic findings(5) and demonstrate that inhibiting VEGF$_{165}$ affected osteolytic bone destruction.

The major pathway for tumor-induced bone lysis involves osteoclast differentiation and activation. Osteoblast dysfunction with increased secretion of matrix metalloproteinases has also been shown to contribute to increased osteolysis. We therefore determined the presence of osteoclasts in the tumor sections by tartrate-resistant acid phosphatase (TRAP) staining. TRAP-positive osteoclasts at the intersection of normal bone and tumor in tibias injected with TC71 or TC/si-control cells were demonstrated (Figure 1A). By contrast, TRAP-positive cells were rarely visible in tibias from mice injected with TC/siVEGF$_{7-1}$ cells. These data suggest

that inhibition of $VEGF_{165}$ by siRNA inhibited osteolysis induced by TC71 cells through inhibition of osteoclast formation.

rhVEGF induced osteoclast formation in vitro

To further investigate the relationship between $VEGF_{165}$ and osteoclast formation, total murine bone marrow cells that contained osteoblasts were cultured with or without rhVEGF. rhM-CSF was used as positive control. After 9 days, TRAP staining was performed to quantify osteoclast formation. Consistent with previous studies, both rhM-CSF and $rhVEGF_{165}$ induced osteoclast differentiation and formation from total bone marrow cells (Figures 1B, 1C). In order to determine whether $rhVEGF_{165}$ had a direct effect on osteoclasts or required the presence of osteoblasts to induce osteoclast formation like many other osteogenic factors, non-adherent murine bone marrow cells in which osteoblasts were eliminated, as described in Materials and Methods, were cultured with or without MC3T3-E1 murine osteoblasts in the presence of rhM-CSF or $rhVEGF_{165}$. rhM-CSF failed to induce osteoclast differentiation without MC3T3-E1 osteoblast cells (Figure 1D). By contrast, rhVEGF alone was able to support osteoclast formation. These data indicate that $rhVEGF_{165}$ can induce osteoclast formation by acting on osteoclast precursor cells.

Effect of VEGF on RANKL expression

Many osteogenic factors and hormones are known to regulate osteoclast formation through the regulation of RANKL expression on osteoblasts and bone marrow stromal cells. Osteoclast precursors express RANK. Therefore, increasing the expression of RANKL on osteoblasts will increase the potential interaction of the ligand and receptor and favor osteoclast differentiation. We investigated whether VEGF induced RANKL expression. An increase in RANKL RNA and protein was seen in MC3T3-E1 osteoblast cells following incubation with VEGF (Figures 2A, B). The induction of RANKL was not as significant in the bone marrow cells (Figure 2C). To determine if the increased RANKL expression induced by VEGF was mediated by an effect on the RANKL promoter, MC3T3-E1 osteoblast cells were transiently transfected with either a luciferase reporter vector driven by the RANKL promoter or a control-luciferase vector. The cells were cultured with rhVEGF 48 h after transfection for various time periods. A significant increase in RANKL promoter activity was demonstrated 24 h following exposure to rhVEGF (Figure 2D).

We next determined the level of RANKL protein in the various TC71 cell lines. Cell lysates were prepared from TC71, TC/si-control, and the $VEGF_{165}$-inhibited $TC/siVEGF_{7-1}$ and $TC/siVEGF_{7-17}$ cells. Western blot analysis was performed using anti-human RANKL antibody. RANKL protein was detected in TC71 and TC/si-control cells, but was significantly decreased in the $VEGF_{165}$-inhibited $TC/siVEGF_{7-1}$ and $TC/siVEGF_{7-17}$ cells (Figure 3A). RANKL protein increased in a time- and dose-dependent manner in $TC/siVEGF_{7-1}$ cells following incubation with $rhVEGF_{165}$ (Figures 3B and 3C).

$VEGF_{165}$ upregulates RANK expression in osteoclast precursor cells

Osteoclast differentiation is stimulated following the interaction of RANKL released from bone marrow stromal cells or osteoblasts with RANK on osteoclast precursor cells. We next determined if $VEGF_{165}$ was able to induce RANK expression in osteoclast precursor cells. Serum-starved murine osteoclast RAW246.7 cells were cultured with or without $rhVEGF_{165}$ or rhM-CSF. RNA was purified and RANK expression was determined by RT-PCR using specific primers for mouse RANK. RANK expression in RAW246.7 cells increased to 1.67-fold following incubation with rhVEGF, and 1.2-fold following incubation with rhM-CSF as compared with non-stimulated cells (Figure 4).

EWS/FLI-1 regulated RANKL expression through an affect on the promoter

EWS/FLI-1 fusion protein is the specific oncoprotein for Ewing's sarcoma. TC71 cells contain the EWS/FLI-1 fusion protein and express RANKL (Figure 3A). To determine whether EWS/FLI-1 influences RANKL expression we transfected NIH 3T3 cells with EWS/FLI-1 full-length cDNA. RANKL expression was increased following transfection (Figure 5A). Next, a siRNA to EWS/FLI-1 was transfected into TC71 cells. TC71/EWS$_{si}$ cells demonstrated decreased expression of EWS/FLI-1 and RANKL (Figure 5B). The effect of EWS/FLI-1 on the RANKL promoter was determined by cotransfecting cells with EWS/FLI-1 and a RANKL promoter-driven luciferase vector. Luciferase activity was increased after cotransfection of EWS/FLI-1 and RANKL promoter-driven luciferase reporter vector compared to cells cotransfected with a control plasmid and the RANKL promoter-driven luciferase vector (Figure 5C). These data suggest that EWS/FLI-1 may regulate the expression of RANKL through an action on its promoter. Analysis of the 1.9 kb region upstream of the RANKL transcription starting site revealed 9 ETS binding sites. A series of deletion constructs were created in which the ETS binding sites were removed one by one (Figure 5D). These deletion constructs were then transiently transfected into MT3T3-E1 cells with the EWS/FLI-1 expressing plasmid. Deletion of binding sites 8 and 9 drastically reduced luciferase activity to approximately 10% of the full-length RANKL promoter activity. These data suggest that binding sites 8 and 9 are important for the upregulation of RANKL by EWS/FLI-1. Deletion of a region around ETS binding site 4 increased promoter activity (Figure 5D) suggesting a negative regulating region.

Discussion

The data presented demonstrate that VEGF induced osteoclast formation and tumor-induced osteolysis. This activity may be secondary to the upregulation of RANKL on osteoblasts, bone marrow stromal cells and the tumor cells as well as upregulation on RANK on osteoclasts. Inhibition of VEGF$_{165}$ using siRNA lowered RANKL expression and decreased tumor-induced osteolytic bone damage. The upregulation of RANKL by VEGF was transcriptionally regulated by an effect on the RANKL promoter.

VEGF plays a pivotal role in neovascular formation. High VEGF expression has been demonstrated in Ewing's sarcoma cell lines and patient tumor specimens (5). Serum levels of VEGF have been shown to correlate with the prognosis of Ewing's sarcoma patients (16). High levels of VEGF have also been reported in patients with breast cancer metastases to bone (17). Furthermore angiostatin, an angiogenesis inhibitor, markedly inhibited osteolysis induced by breast cancer metastases to the bone(18). Our previous studies have demonstrated that Ewing's sarcoma cells overexpress VEGF with a shift in isoform production from the 189 membrane-bound form to the soluble 165 isoform (4). When injected into the tibia of mice, these cells form lytic tumors, inhibiting VEGF$_{165}$ in inhibited tumor growth and decreased lytic bone destruction (5). Replacement of VEGF$_{165}$ rescued tumor growth and restored tumor-induced bone lysis (19). The mechanism of tumor induced bone lysis was unclear. In this study, we demonstrated that VEGF stimulated osteoclast formation *in vitro* from bone marrow cells with or without the help of osteoblasts. This finding is consistent with previous reports that show that the injection of rhVEGF increased the number of TRAP-positive cells in inflamed joints(20). VEGF has also been reported to support osteoclast bone resorption in op/op mice (21). Blocking VEGF with a chimeric protein not only inhibited tumor vascularity, but also suppressed the formation of osteolytic lesions by acting directly on osteoclast precursor cells (22). Taken together, these data indicate that VEGF participates in tumor-induced osteolysis.

Our data also suggest that bone lysis induced by VEGF is mediated through an effect on the RANK/RANKL pathway. The RANK/RANKL/OPG triad has been shown to regulate normal and cancer-induced osteoclastogenesis. Many of the factors that regulate osteoclastogenesis increase expression of RANKL (23). Prostate cancer, myeloma and T-cell leukemia cells have

been shown to induce RANKL expression. Tumor-derived fibroblasts and bone marrow stromal cells from Ewing's sarcoma tumors were shown to express RANKL. These cells were capable of inducing osteoclast formation (24). Our data is consistent with these findings, as we demonstrated RANKL expression in human TC71 Ewing's sarcoma cells. The expression of RANKL by tumor cells and osteoblasts was upregulated by rhVEGF while inhibiting $VEGF_{165}$ by specific siRNA resulted in decreased RANKL.

The high expression of RANKL in TC71 cells may be attributed to the EWS/FLI-1 translocation, the hallmark of Ewing's sarcoma. The EWS/FLI-1 fusion protein is expressed in TC71 cells. This oncoprotein is a transcription factor that has been shown to stimulate the VEGF promoter by interacting with a Sp1 binding site (25). Our data demonstrate that transfection of NIH 3T3 cells with EWS/FLI-1 upregulated RANKL via an effect on the RANKL promoter (Figures 5A and 5C). Analysis of the 1.9 kb promoter region of the human RANKL gene revealed 9 ETS binding sites. Serial deletion of each binding site demonstrated that site 8 is responsible for the enhanced transcriptional regulation of RANKL by EWS/FLI-1. Our data also suggest that 1 or more binding sites may exist around site 4 or site 5 of the RANK promoter as deletion of this region resulted in a 2-fold increase in luciferase activity. Transfection of EWS/FLI-1 siRNA into TC71 cells resulted in decreased EWS/FLI-1 expression and decreased RANKL consistent with our results using NIH 3T3 cells (Figure 5B). It is possible that the effect of EWS/FLI-1 on RANKL may be indirect and secondary to its transcriptional regulation of VEGF. Future studies will be aimed at dissecting these 2 factions.

In summary, we have demonstrated that VEGF acts on multiple cell types, including osteoblasts, bone marrow stromal cells, osteoclasts and Ewing's sarcoma cells to upregulate RANK and RANKL expression and stimulate osteoclast formation. We conclude that VEGF plays an important role in osteolytic bone damage in addition to its critical role as an angiogenic agent. Targeting VEGF may, therefore, be a benefit on 2 fronts: blocking tumor vascular formation and reducing bone lysis, which may significantly impact bone pain. Our data support the concept of using anti-VEGF therapy for the treatment of Ewing's sarcoma patients and perhaps patients with bone metastases from other tumors. It behooves us to consider such a novel therapeutic approach as the outcome for Ewing's sarcoma patients has not changed for over 20 years.

Acknowledgments

References

1. Riggi N, Stamenkovic I. The Biology of Ewing sarcoma. Cancer Lett 2007;254:1–10. [PubMed: 17250957]

2. Rodriguez-Galindo C, Spunt SL, Pappo AS. Treatment of Ewing sarcoma family of tumors: current status and outlook for the future. Med Pediatr Oncol 2003;40:276–287. [PubMed: 12652615]

3. Dvorak HF. Vascular permeability factor/vascular endothelial growth factor: a critical cytokine in tumor angiogenesis and a potential target for diagnosis and therapy. J Clin Oncol 2002;20:4368–4380. [PubMed: 12409337]

4. Lee TH, Bolontrade MF, Worth LL, Guan H, Ellis LM, Kleinerman ES. Production of VEGF165 by Ewing's sarcoma cells induces vasculogenesis and the incorporation of CD34+ stem cells into the expanding tumor vasculature. Int J Cancer 2006;119:839–846. [PubMed: 16557578]

5. Guan H, Zhou Z, Wang H, Jia SF, Liu W, Kleinerman ES. A small interfering RNA targeting vascular endothelial growth factor inhibits Ewing's sarcoma growth in a xenograft mouse model. Clin Cancer Res 2005;11:2662–2669. [PubMed: 15814647]

6. Henriksen K, Karsdal M, Delaisse JM, Engsig MT. RANKL and vascular endothelial growth factor (VEGF) induce osteoclast chemotaxis through an ERK1/2-dependent mechanism. J Biol Chem 2003;278:48745–48753. [PubMed: 14506249]

7. Nakagawa M, Kaneda T, Arakawa T, Morita S, Sato T, Yomada T, Hanada K, Kumegawa M, Hakeda Y. Vascular endothelial growth factor (VEGF) directly enhances osteoclastic bone resorption and survival of mature osteoclasts. FEBS Lett 2000;473:161–164. [PubMed: 10812066]

8. Niida S, Kondo T, Hiratsuka S, Hayashi S, Amizuka N, Noda T, Ikeda K, Shibuya M. VEGF receptor 1 signaling is essential for osteoclast development and bone marrow formation in colony-stimulating factor 1-deficient mice. Proc Natl Acad Sci U S A 2005;102:14016–14021. [PubMed: 16172397]

9. Iguchi H, Yokota M, Fukutomi M, Uchimura K, Yonemasu H, Hachitanda Y, Nakao Y, Tanaka Y, Sumii T, Funakoshi A. A possible role of VEGF in osteolytic bone metastasis of hepatocellular carcinoma. J Exp Clin Cancer Res 2002;21:309–313. [PubMed: 12385570]

10. Kumta SM, Huang L, Cheng YY, Chow LT, Lee KM, Zheng MH. Expression of VEGF and MMP-9 in giant cell tumor of bone and other osteolytic lesions. Life Sci 2003;73:1427–1436. [PubMed: 12850503]

11. Lacey DL, Timms E, Tan HL, Kelley MJ, Dunstan CR, Burgess T, Elliott R, Colombero A, Elliott G, Scully S, Hsu H, Sullivan J, Hawkins N, Davy E, Capparelli C, Eli A, Qian Y,X, Kaufman S, Sarosi I, Shalhoub V, Senaldi G, Guo J, Delaney J, Boyle WJ. steoprotegerin ligand is a cytokine that regulates osteoclast differentiation and activation. Cell 1998;93:165–176. [PubMed: 9568710]

12. Yasuda H, Shima N, Nakagawa N, Yamaguchi K, Kinosaki M, Mochizuki S, Tomoyasu A, Yano K, Goto M, Murakami A, Tsuda E, Morinaga T, Higashio K, Udagawa N, Takahashi N, Suda T. Osteoclast differentiation factor is a ligand for osteoprotegerin/osteoclastogenesis-inhibitory factor and is identical to TRANCE/RANKL. Proc Natl Acad Sci U S A 1998;95:3597–3602. [PubMed: 9520411]

13. Weitzmann MN, Cenci S, Rifas L, Haug J, Dipersio J, Pacifici R. T cell activation induces human osteoclast formation via receptor activator of nuclear factor kappaB ligand-dependent and -independent mechanisms. J Bone Miner Res 2001;16:328–337. [PubMed: 11204433]

14. Zhang J, Dai J, Qi Y, Lin DL, Smith P, Strayhorn C, Mizokami A, Fu Z, Westman J, Keller ET. Osteoprotegerin inhibits prostate cancer-induced osteoclastogenesis and prevents prostate tumor growth in the bone. J Clin Invest 2001;107:1235–1244. [PubMed: 11375413]

15. Tropel P, Noel D, Platet N, Legrand P, Benabid AL, Berger F. Isolation and characterisation of mesenchymal stem cells from adult mouse bone marrow. Exp Cell Res 2004;295:395–406. [PubMed: 15093739]

16. Holzer G, Obermair A, Koschat M, Preyer O, Kotz R, Trieb K. Concentration of vascular endothelial growth factor (VEGF) in the serum of patients with malignant bone tumors. Med Pediatr Oncol 2001;36:601–604. [PubMed: 11344490]

17. Aldridge SE, Lennard TW, Williams JR, Birch MA. Vascular endothelial growth factor receptors in osteoclast differentiation and function. Biochem Biophys Res Commun 2005;335:793–798. [PubMed: 16105658]

18. Peyruchaud O, Serre CM, NicAmhlaoibh R, Fournier P, Clezardin P. Angiostatin inhibits bone metastasis formation in nude mice through a direct anti-osteoclastic activity. J Biol Chem 2003;278:45826–45832. [PubMed: 12954626]

19. Zhou Z, Reddy K, Guan H, Kleinerman ES. VEGF(165), but not VEGF(189), stimulates vasculogenesis and bone marrow cell migration into Ewing's sarcoma tumors in vivo. Mol Cancer Res 2007;5:1125–1132. [PubMed: 18025258]

20. Ren WP, Markel DC, Zhang R, Peng X, Wu B, Monica H, Wooley PH. Association between UHMWPE particle-induced inflammatory osteoclastogenesis and expression of RANKL, VEGF, and Flt-1 in vivo. Biomaterials 2006;27:5161–5169. [PubMed: 16814378]

21. Kodama I, Niida S, Sanada M, Yoshiko Y, Tsuda M, Maeda N, Ohama K. Estrogen regulates the production of VEGF for osteoclast formation and activity in op/op mice. J Bone Miner Res 2004;19:200–206. [PubMed: 14969389]

22. Akiyama H, Mohamedali KA, Kachi S, Shen J, Hatara C, Umeda N, Hackett SF, Aslam S, Krause M, Lai H, Rosenblum MG, Campochiaro PA. Vascular targeting of ocular neovascularization with

a vascular endothelial growth factor121/gelonin chimeric protein. Mol Pharmacol 2005;68:1543–1550. [PubMed: 16150930]

23. Dougall WC, Chaisson M. The RANK/RANKL/OPG triad in cancer-induced bone diseases. Cancer Metastasis Rev 2006;25:541–549. [PubMed: 17180711]

24. Lau YS, Adamopoulos IE, Sabokbar A, Giele H, Gibbons CL, Athanasou NA. Cellular and humoral mechanisms of osteoclast formation in Ewing's sarcoma. Br J Cancer 2007;96:1716–1722. [PubMed: 17533390]

25. Fuchs B, Inwards CY, Janknecht R. Vascular endothelial growth factor expression is upregulated by EWS-ETS oncoproteins and Sp1 and may represent an independent predictor of survival in Ewing's sarcoma. Clin Cancer Res 2004;10:1344–1353. [PubMed: 14977835]
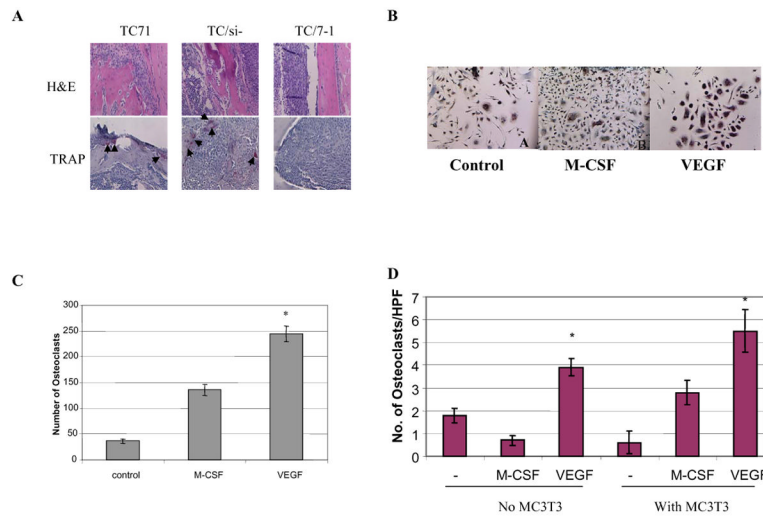
Figure 1.
Effect of VEGF on TC71 tumor phenotype and osteoclast formation. (**A**) TC71, TC/si-control, or TC/siVEGF$_{7-1}$ cells were injected into the tibia of nude mice. Bone tumors were removed after 3 weeks and assessed by H&E staining. The presence of osteoclasts was determined by TRAP staining (arrows). (**B**) Murine bone marrow cells were cultured with rhVEGF or rhM-CSF for 9 days. Osteoclast formation was assessed by TRAP staining. (**C**) TRAP-positive multinuclear cells were quantified by light microscopy. (**D**) Suspended murine bone marrow cells were cultured with rhVEGF or rhM-CSF in the presence or absence of murine osteoblast MC3T3-E1 cells. TRAP-positive multinuclear cells were then quantified. Results are the mean ± SE of 3 separate experiments ($P<0.05$).
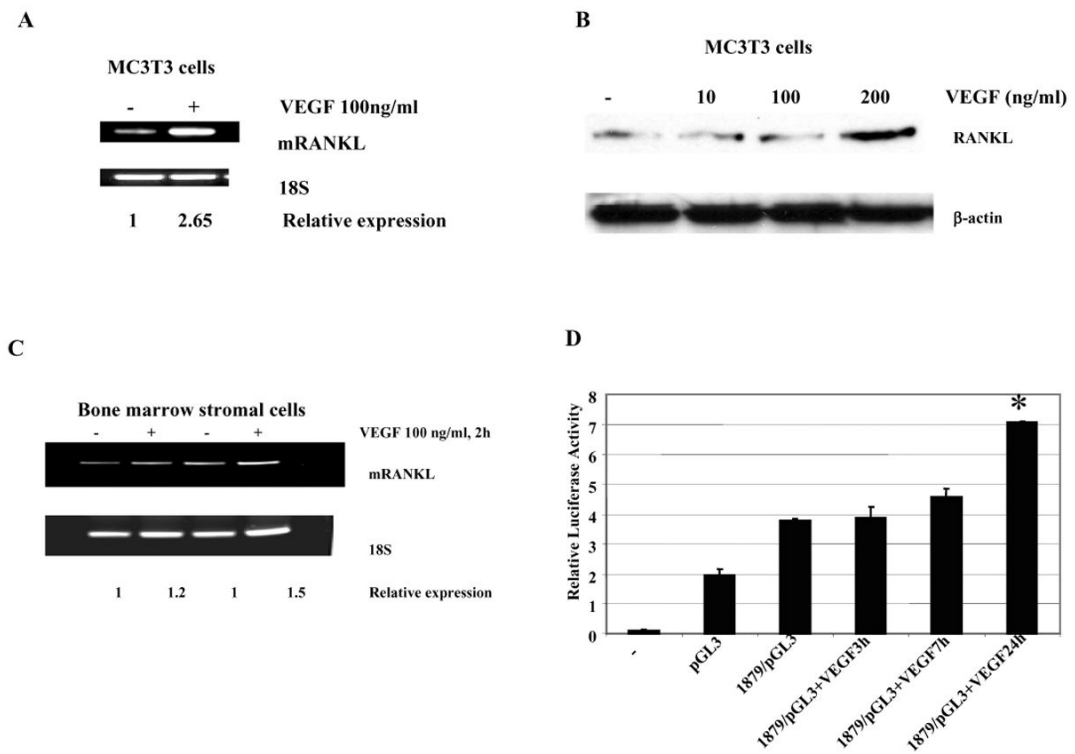
Figure 2.
Effect of VEGF on RANKL expression in murine bone marrow stromal cells and osteoblasts. Serum-starved murine bone marrow stromal cells (**A**) or MC3T3-E1 murine osteoblast cells (**B**) were cultured with rhVEGF 100 ng/ml for 2 h. Total RNA was extracted, and RANKL expression was quantified by RT-PCR. (**C**) MC3T3-E1 murine osteoblast cells were cultured with rhVEGF at different concentrations for 24 h. RANKL protein level was quantified by Western blot analysis. (**D**) MC3T3-E1 cells were transfected with 1 μg of RANKL/Luc reporter plasmid plus 50 ng of Renilla-luc expression vector. Twenty-four h after transfection, cells were serum starved overnight and then stimulated with rhVEGF 100 ng/ml for 3, 7, and 24 h. Luciferase activity was determined. Results are expressed as relative luciferase activity normalized to Renilla luciferase activity from the transfection control plasmid and represent the mean value ± SE from 3 experiments ($P<0.05$).

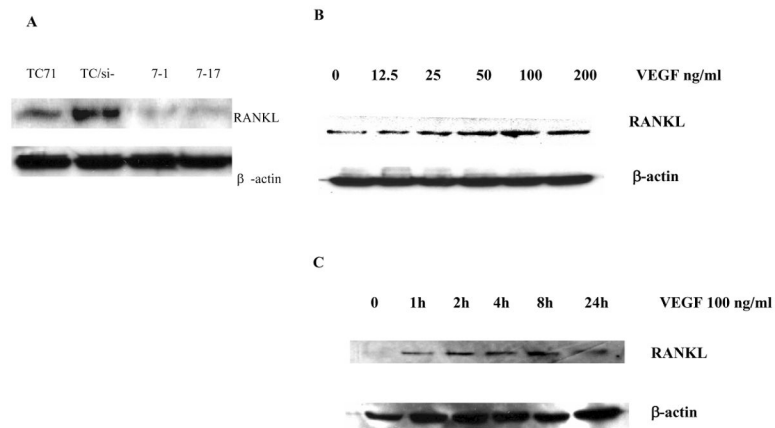**Figure 3.**
Effect of VEGF on RANKL expression in TC71 parental and transfected cells. (**A**) Cell lysates were extracted from TC71, TC/si-, TC/siVEGF$_{7-1}$ and TC/siVEGF$_{7-17}$ cells and assayed by Western blot analysis using anti-human RANKL antibody. β-actin was used as the internal control. (**B, C**) Serum-starved TC/siVEGF$_{7-1}$ cells were cultured with (**B**) various concentrations of rhVEGF for 24 h, or (**C**) with rhVEGF at 100 ng/ml for different time points. Cell lysates were collected and assayed by Western blot analysis.
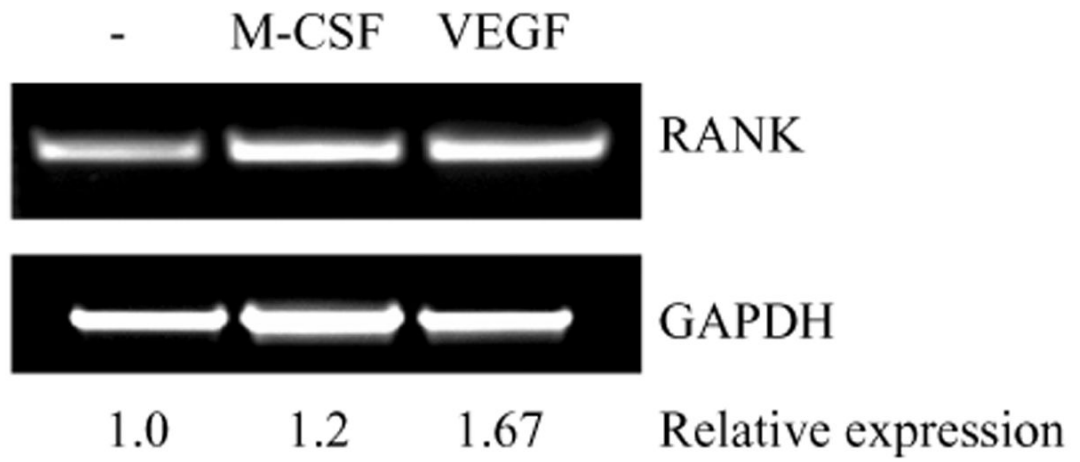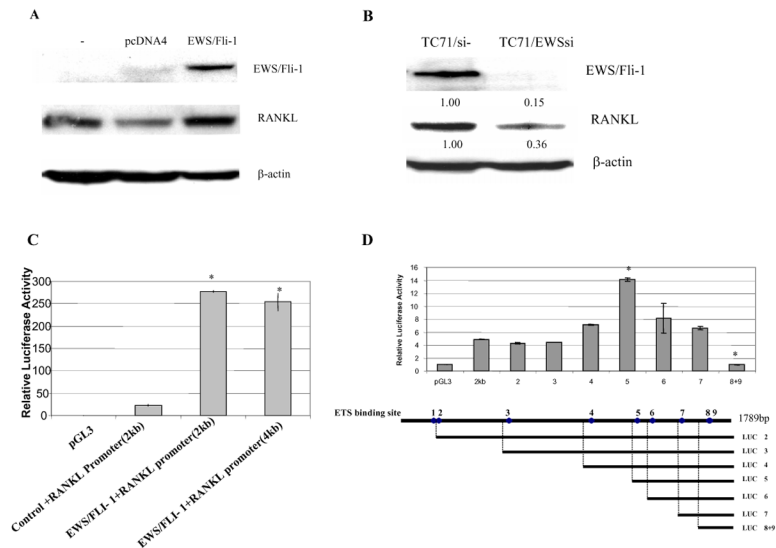
Figure 4.
VEGF upregulates RANK. (**A**) Serum starved RAW246.7 cells were cultured with rhVEGF at 100ng/ml for 2 h. RANK expression was determined by RT-PCR.

Figure 5.
EWS/FLI-1 regulates RANKL expression in TC71 Ewing's sarcoma cells. (**A**) Murine fibroblast NIH3T3 cells were stably transfected with EWS/FLI-1 expression plasmid. RANKL protein level was determined by Western blot analysis. β-actin was the internal control. (**B**) TC71 cells were transiently transfected with EWS/FLI-1 siRNA. RANKL protein levels were determined by Western blot analysis following transfection. (**C**) NIH 3T3 cells were transfected with pGL3 luciferase vector (control), or RANKL promoter/luc vector (RANKL promoter 2 kb or 4 kb), with or without cotransfection of EWS/FLI-1-expression plasmid. Cell lysates were collected 24h later and luciferase activity quantified. (**D**) Serial deletion RANKL promoter plasmids were constructed. NIH 3T3 cells were co-transfected with EWS/FLI-1 expressing plasmid and pGL3 luciferase reporting plasmid, RANKL-luciferase plasmid or one of serial deletion constructs. Cell lysates were collected 24 h later and luciferase activity quantified.